DOR: 20.1001.1.27170314.2023.12.1.2.5

Research Paper

Numerical and Experimental Comparison of Flow Stress and the Effect of Microcylinder Topography in the Barreling Test: An Artificial Neural Network Model

Mohammad Honarpisheh[1*], Narges Shooshtari[2]
[1]Faculty of Mechanical Engineering, University of Kashan, Kashan, Iran
[2]University of Kashan, Kashan, Iran
[*]Email of Corresponding Author: honarpishe@kashanu.ac.ir
Received: January 3, 2023; Accepted: February 21, 2023

Abstract
In any case, macroscale shaping cannot be transferred to microscale due to the size effect. There are different parameters to evaluate small-scale forming. In this article, the effect of flow stress and topography in two states of lubrication and without lubrication for T2 copper micro cylinder has been investigated using the numerical solution and prediction of a trained neural network. An artificial neural network model has been presented to investigate the flow stress and the effect of friction with the miniaturization of the copper microcylinder. The results show that the flow stress decreases with decreasing the initial specimen diameter in both lubrication conditions, and the flow stress decreases by 30 MPa with the initial specimen diameter decreasing from 8 mm to 1 mm. The friction factor increases obviously with decreasing the initial specimen diameter in the case of lubricating with castor oil, and the friction factor increases by 0.11 with the initial specimen diameter decreasing from 8 mm to 1 mm. However, the tribology size effect is not found in the case without lubrication. The reasons for the flow stress and tribology size effects were also discussed. The good matching of outputs and objectives in the regression graphs shows that the response of the neural network is satisfactory.

Keywords
Microcylinder, Tribology, Flow Stress, FEM, Neural Network

1. Introduction

Due to their small size and structure, micro parts have different physical, mechanical, and metallurgical properties than macro structures. The production of micro parts is one of the innovation movements in many new products, including the production of new models of computers, cars, mobile phones, CD players, MP3 players, and a range of flat screens, medical tools, implants, etc. [1]. Micro forming is one of the most popular ways to form small parts due to mass production, high efficiency, high precision, short duration, low cost, and no pollution. Although the metal-forming process is well understood and widely used, micro-forming is unwise due to size effects directly. Although the effect of the flow stress size has become one of the focuses of research in micro forming in these years, most researchers have focused on micro metal forming. The size effect in the formation

of micro-sheets has been widely investigated in stress [2-3], bending [4-5], and tensile processes [6-7], and almost no explanations are available. However, only some studies focused on extensive microformat. Messener et al. [8] and Chen et al. [9] investigated the effect of flow stress size of copper-zinc alloy using fracture and microhardness tests, respectively, and showed that the flow stress decreases with the reduction of sample dimension. Compared to the size effect of flow stress, research on the size effect of tribology was limited. Messener and his colleagues [8] for the first time investigated the effect of tribological size using a cylinder pressure test and showed that the coefficient of friction increased by decreasing the initial size of the sample. Nanthakumar et. al [10] studied two extrusion cups and found that friction increases dramatically under miniaturization with lubrication, but friction is constant without lubrication. Ghassemali et. al [11] manufactured micro-pins through a novel progressive micro-forming process. However, Krishnan et al. [12] found that by reducing the size of the extruded pins in microextrusion without lubrication, the coefficient of friction decreases. Vollertsen et. al [13-14] macro tension and studied micro and developed a new friction test method to study the size effect of tribology, the results showed that the coefficient of friction in micro forming is much higher than macro forming. This research aims to develop an artificial neural network model for predicting flow stress with changes in friction coefficients in both lubricated and non-lubricated conditions. The coefficient of friction has a major effect on the drawing force and the wall thickness reduction [15]. Many advances in the development of intelligent systems are inspired by biological neural networks. It has been achieved. Artificial neural networks are used for information processing. Cylindrical compression is a common method to obtain the stress-strain curve and it is also a simple method to determine the friction factor in metal forming. In this research, low-scale cylinder compression has been done to investigate the amount of flow stress and the size of the effect of tribology in micro-forming. The subject of this research is to investigate and compare the compressibility of the effect of friction in two states of lubrication and without lubrication of 4 micro-cylinders of different sizes using a numerical solution and neural network model, finally the results of a numerical solution with a similar article [16-17]. The results of the experimental solution have been compared. The results of the two numerical and experimental solutions show the same compliance. Recently, the severe plastic deformation processes (SPD) such as equal channel angular pressing (ECAP) [18], equal channel angular rolling (ECAR) [19, 20], high-pressure tube twisting (HPTT) [21], constrained groove pressing (CGP) [22, 23], non-equal-channel angular pressing (NECAP) [24, 25] and cyclic close die forging (CCDF) [26-28] have been used in the micro forming fields. These techniques are particularly suited for the micro-forming of metals. For example, Supriadi et. al [29] used the ECAP process as a micro-forming process to form the mini plate.

Considering that a lot of research has been done in the field of a copper microcylinder, the study of the effect of surface mapping is limited in the sources and the presentation of the neural network model in this regard has not been reported in the sources. In this study, four T2 copper micro cylinders with diameters of 1, 2, 4, and 8 mm were examined in the microbarrelization test (Figure 1). The triaxial flow stress has been simulated in friction conditions between the microplate and the cylinder piece. Since the Johnson cook model is more for investigating the effect of flow stress, in this research, the effect of barreling is also simulated under the J-C model. The form and size of the samples were prepared according to the Chinese standard GB/T 73142005. Copper micro-cylinders have been simulated with ABAQUS software at a temperature of 400ºC under annealing conditions.

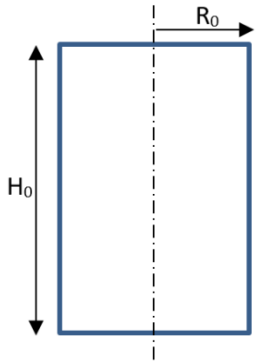

Figure 1. Microcylinder before micro forming

2. Neural network model

The purpose of an artificial neural network is to extract patterns and recognize trends from complex or ambiguous data. There are different methods to train the neural network, a neural network consists of several inputs, hidden, and output layers. These networks come in various forms, from forward synthetic networks, backpropagation, and radial basis function network. The training of the artificial neural network begins with the selection of a random weight function. These functions are adjusted so that the error reaches its minimum value [30-31]. The weighting function of artificial neural cells with a back propagation algorithm is as follows [32-33]:

$$A_k = b_k \sum_{j=1} W_{kj} X_j \quad (1)$$

Where Wkj is the weight of the interface between neuron cell k and neuron j, Ak is the weighted input of cell k, bk is the base and Xj is the input signal. As can be seen, activation only depends on input and weight. The output from the hidden layers Yk is defined using the sigmoid transfer function:

$$Y_k = \frac{1 - e^{A_k}}{1 + e^{A_k}} \quad (2)$$

A linear function is used to calculate the output from the output layer:

$$Y_1 = \frac{1\text{-}e^{A_1}}{1+e^{A_1}} \, , A_1 = b_1 + \sum_{k=1}^{p} W_{kj} x_j \quad (3)$$

Where p is the number of hidden layer cells. Indices l, j, k refers to hidden input and output layers, respectively. The use of ten neural cells in the hidden layer provides a good match between the results of finite components predicted by the neural network. As a result, this configuration is chosen for neural network training. This network has an input layer including the effect of friction and flow stress in the output layer. Matlab ANN toolbox is used to build the neural network. Program input data is entered as a vector. In the Matlab software toolbox, the divider and option are used, in which a percentage of data is randomly selected for validation and a percentage for network testing. In this work, 15% of validation and 15% are used for network testing and the rest of the data are used for network training.

3. Finite element model

In this method of micro forming behavior, the effect of friction in two cases of lubrication and without lubrication is modeled with the help of the Johnson-Cook relationship [31].

$$\sigma_y=(A+B\varepsilon^n)\left(1+C\ln\frac{\dot{\varepsilon}_{eq}^{p}}{\dot{\varepsilon}_0}\right)\left(1-\left(\frac{T-T_r}{T_m-T_r}\right)^m\right) \quad (4)$$

$$\varepsilon=\ln(H/H0-\Delta H) \quad (5)$$

$$\sigma=P/A0\exp\varepsilon \quad (6)$$

In this equation, σy is the true stress, ε is the true plastic strain, $\dot{\varepsilon}_0$ plastic strain rate, $\dot{\varepsilon}_{eq}^{p}$ is the base plastic strain rate, T is the instantaneous temperature of the workpiece, Tr is the ambient temperature, Tm is the melting temperature of the workpiece material, and m, n, B, and A constant are in this equation.

4. Calculation of strain stress and friction factors

The flow stress and true strain are checked according to the following relations:

$$m=\frac{\left(\frac{R}{H}\right)b}{\left(\frac{4}{\sqrt{3}}\right)-(2b/3\sqrt{3})} \quad (7)$$

$$b=4\frac{\Delta R}{R}*\frac{H}{\Delta H} \quad (8)$$

$$R=R_0\sqrt{H_0/H} \quad (9)$$

$$R_T=\sqrt{\left(\frac{3H_0}{H}R_0^2\right)-2R_M{}^2} \quad (10)$$

So that ε is the true strain, H0 is the initial height of the microcylinder, ΔH is the reduction in the height of the microcylinder after forming, σ is the flow stress, P is the applied pressure in the microcylinder, and A0 is the initial cross-section of the microcylinder. Due to the presence of high friction in the mold, the micro cylinder becomes a barrel after forming. The friction coefficient follows the following relations under the upper limit relations:

m is the friction factor, R is the average radius of the micro cylinder after forming, H is the height of the micro cylinder after forming, and b is the barreling parameter (Figure 2).

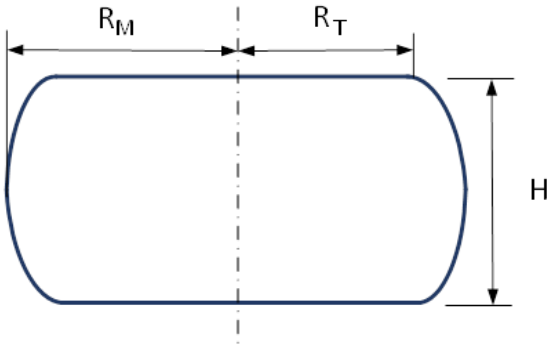

Figure 2. Micro-cylinder after micro-shaping [16]

Flow stress diagram - the true strain of different micro samples is shown in the figure. The flow stress of micro cylinders can be obtained based on the true strain-flow stress diagram. According to the

experimental test [16], the flow stress has been reduced by reducing the diameter of the micro cylinders from the value of 30 MPa, these values are shown in Table 1. The results of the calculation of flow stress-true strain are the same in both experimental and numerical conditions (Figure 3). This result shows the effect of the size effect on the flow stress in both lubrication and non-lubrication conditions in micro parts (Figure 4).

Table 1. the tension of the currents obtained from the laboratory solution.

diameter (μm)	flow stress lubrication (MPa)	flow stress non-lubrication (MPa)
1000	30	30
2000	45.2	30.2
4000	50.8	30.28
8000	67	30.8

5. Flow stress size effect

During scaling down of the size of the material to the micron level only a very small amount of grain participates in forming operation and therefore the position, orientation, and size of the individual grain are very important. Due to the inhomogeneous nature of materials, scattering of process parameters occurs such as scattering of flow stress, which affects the formability of the process. Therefore, a solution to this problem was to conduct micro-forming operations at elevated temperatures which will bring back homogeneous nature to the material and limit the scattering of process parameters. The micro-manufacturing process at elevated temperature was carried out at copper alloy from room temperature to 400 C to limit the scattering of parameters. Enlargement in forming limit, reduced required forming load, and decrease in flow stress scattering were observed during the process which implies the use of elevated temperature operations to benefit in reducing the inhomogeneity of materials during micro forming operations. Table 2 shows the comparison of the results of flow stress on a sample size of different materials.

Table 2. Comparing the results of flow stress on the grain size of different materials

diameter (μm)	flow stress (MPa)	Material
10000	70	AL1100-Brass [34]
1000	30	AL1100- Brass
2000	80	Pure Nickel [35]
1000	65	Pure Nickel
8000	67	Copper
1000	30	Copper

The effect of flow stress depends on the size change of micro samples. Since the grains on the surface of the sample have a more noticeable deformation compared to the grain of the depth of the micro cylinder [16], during the forming process, the internal grains accumulate towards the grain boundary. This behavior of the material increases the hardness and resistance of the piece against deformation, as a result, the flow stress of the grains on the surface of the sample is lower than the depth (Figure 3). By reducing the size of the prototype, the ratio of surface grains to grains in the volume increases, and as a result, the applied force decreases (Figure 4).

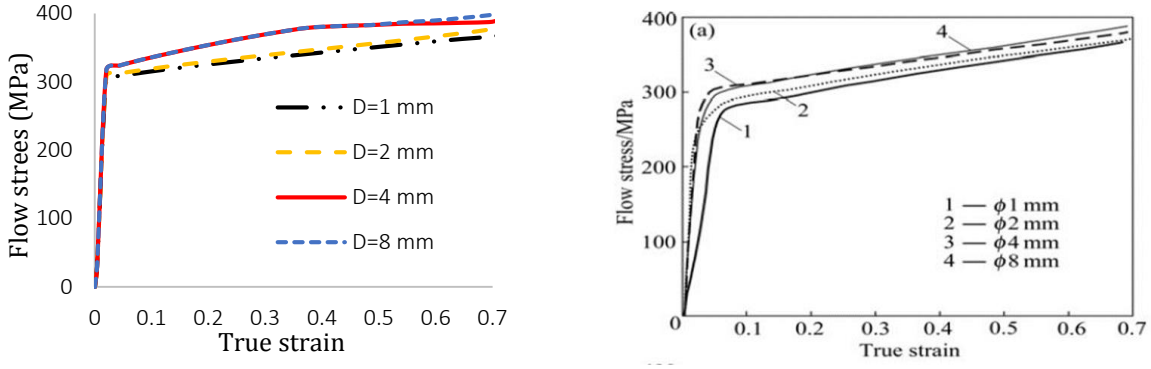

Figure 3. Stress diagram - true strain without lubrication a) simulation b) experimental

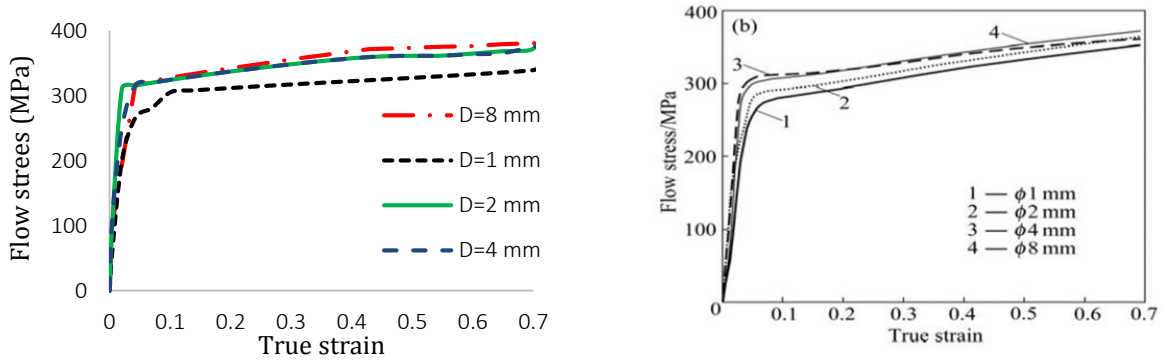

Figure 4. Stress diagram - true strain with lubrication a) simulation b) experimental

The effect of the flow stress size on the process of micro-discharge of the micro-cylinder in two cases of lubrication and without lubrication has been investigated. The yield stress decreases by about 30 MPa because the sample size decreases from 8 mm to 1 mm. This case can be significant by changing the dimensions of the samples. The friction coefficient increases around 0.11 because the size of the sample decreases from 8 mm to 1 mm (Figure 5). LSCM images of the topography of 1 and 4-mm diameter samples are shown in Figures 6 and 7.

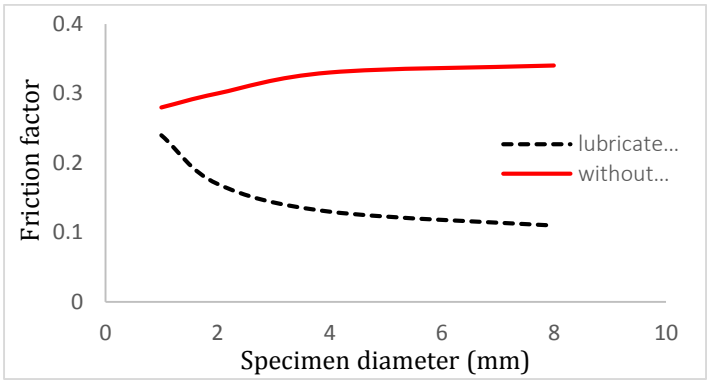

Figure 5. The friction factor of samples with different diameters, laboratory results.

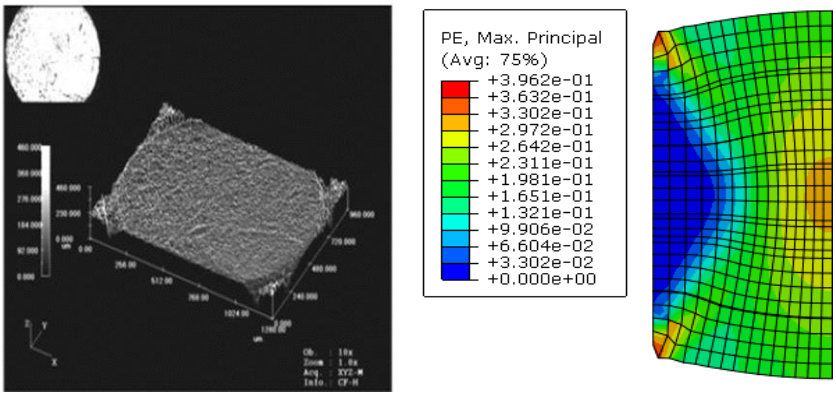

Figure 6. The effect of surface drawing of the simulated 1 mm sample, lubrication.

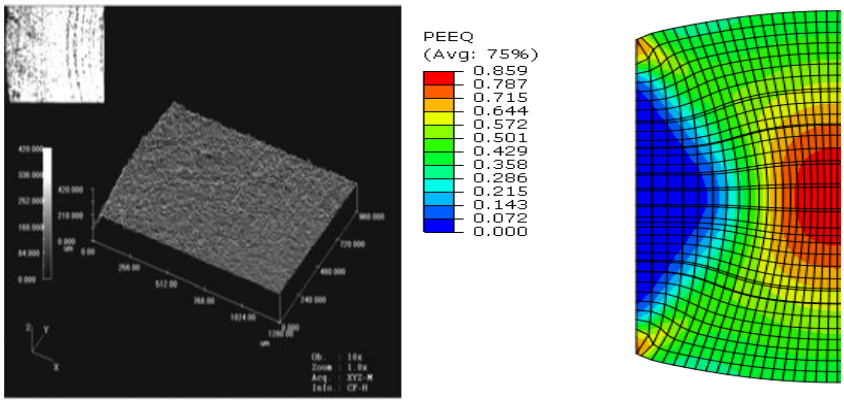

Figure 7. The effect of surface mapping of the simulated 4 mm sample, lubrication.

In the case of lubrication with oil, the effect of micro-compression has been reduced, because, in the case of lubrication, the degree of deformation in the inner part is much lower than the edge, when a forming load is applied to the surface of the workpiece. Lubrication is applied, and the lubricant is removed at the edge and cannot transmit the forming load. The forming load can only be applied on the uneven part and leads to more friction than the actual contact surface. While in the inner part, the lubricant can transfer part of the load, resulting in less contact surface and less friction. However, the effect of topography size is not found in the case without lubrication. This can be achieved by examining the effect of friction in the actual contact area under deformation.

5.1 Tribology size effect

As the tribological conditions between tool and workpiece in metal working are of the greatest importance for process feasibility and process quality this is even more true when the process is scaled from conventional down to micro dimensions. As can be shown by scaled friction tests which will have a distinct impact on all factors characterizing the process. By reducing the actual contact surface, it increases, and the friction on the edge increases. In Figures 8 and 9, only the edges are severely deformed, because the forming load can only be applied to the uneven parts and does not affect a part of the real contact surface, so the effect of surface mapping can be observed in this case. The form regression diagrams show the output according to the data of training, validation, testing, and all prediction sets. The values obtained from finite element analysis are shown as targets on the horizontal axis and network prediction values as outputs on the vertical axis in Figure 10. In these graphs, almost all the data coincide on the diagonal lines, which means that the values predicted by

the neural network and the results of the finite element analysis match. Therefore, the good matching of outputs and goals shows that the response of the network is satisfactory. The standard deviation of R for all data is 1 or close to 1.

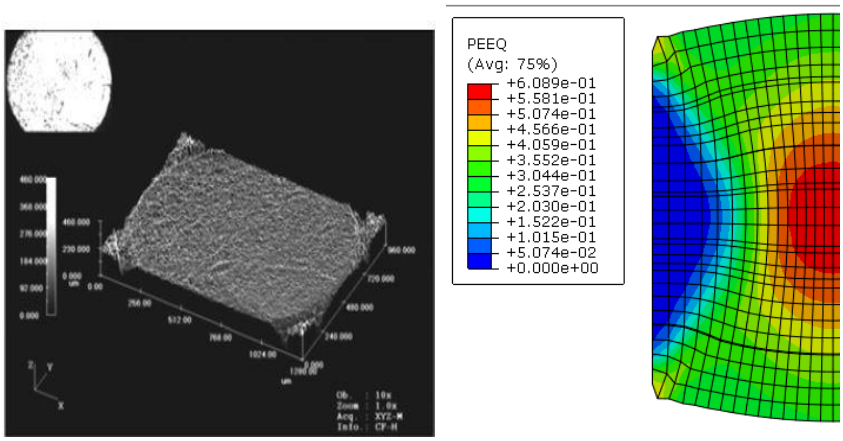

Figure 8. The effect of surface drawing of the simulated 1 mm sample, without lubrication

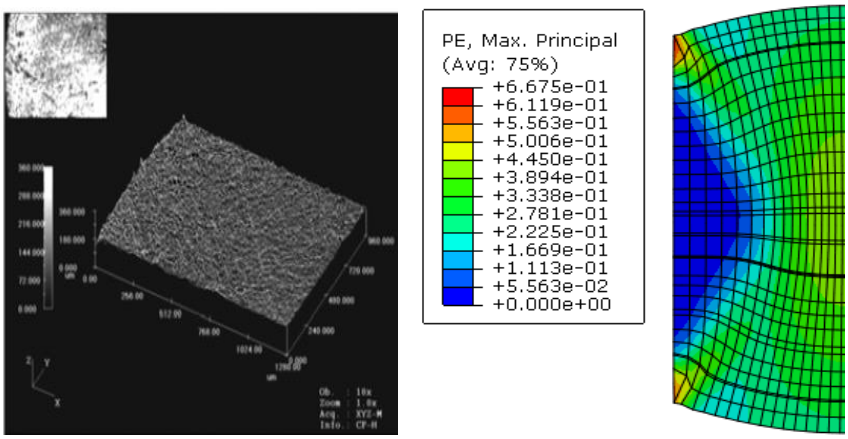

Figure 9. The effect of the simulated 4 mm sample surface, without lubrication

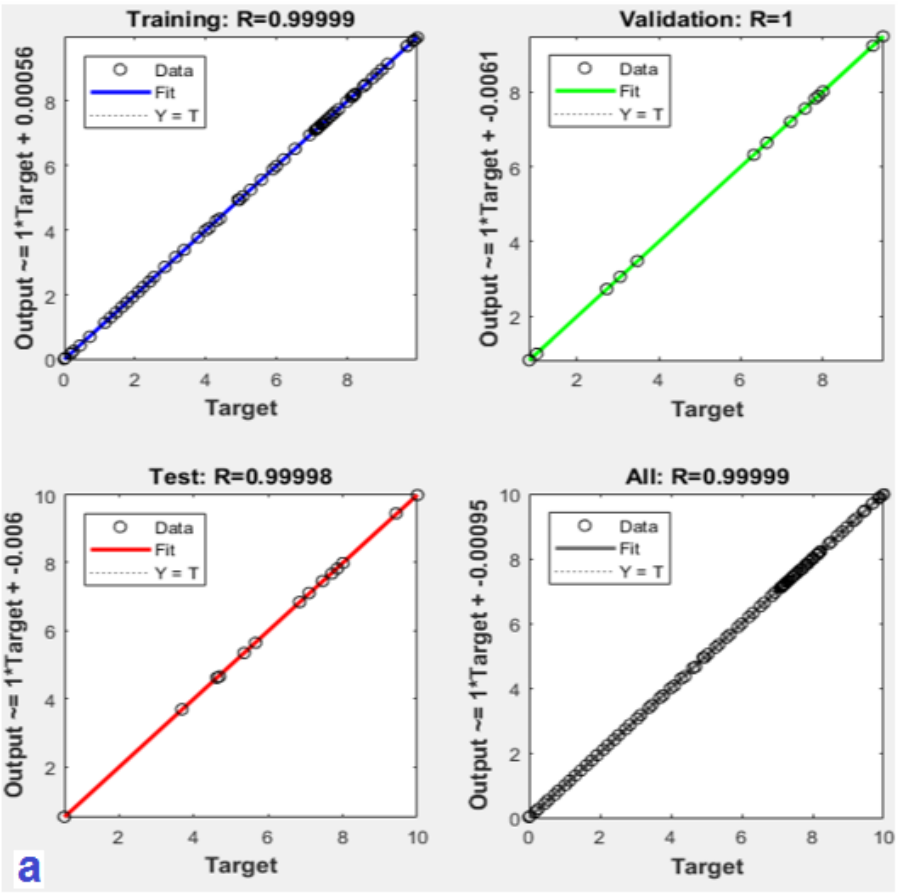
Training: R=0.99999
Validation: R=1
Test: R=0.99998
All: R=0.99999
Data
Fit
Y = T
Target
Output ~= 1*Target + 0.00056
Output ~= 1*Target + -0.0061
Output ~= 1*Target + -0.006
Output ~= 1*Target + -0.00095
a

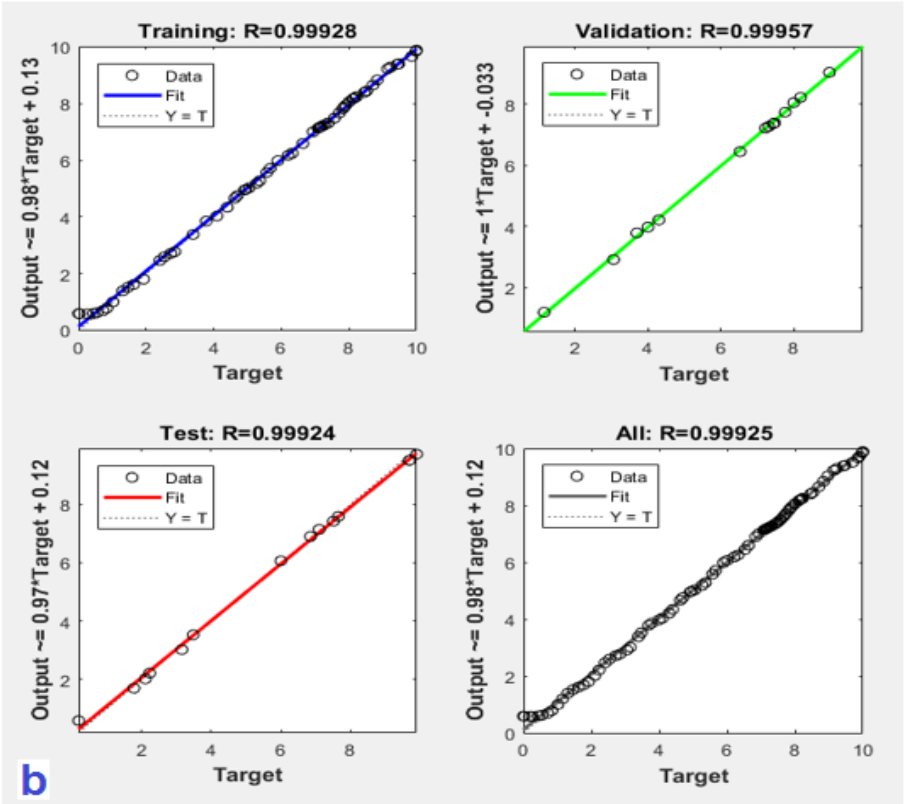
Training: R=0.99928
Validation: R=0.99957
Test: R=0.99924
All: R=0.99925
Data
Fit
Y = T
Target
Output ~= 0.98*Target + 0.13
Output ~= 1*Target + -0.033
Output ~= 0.97*Target + 0.12
Output ~= 0.98*Target + 0.12
b

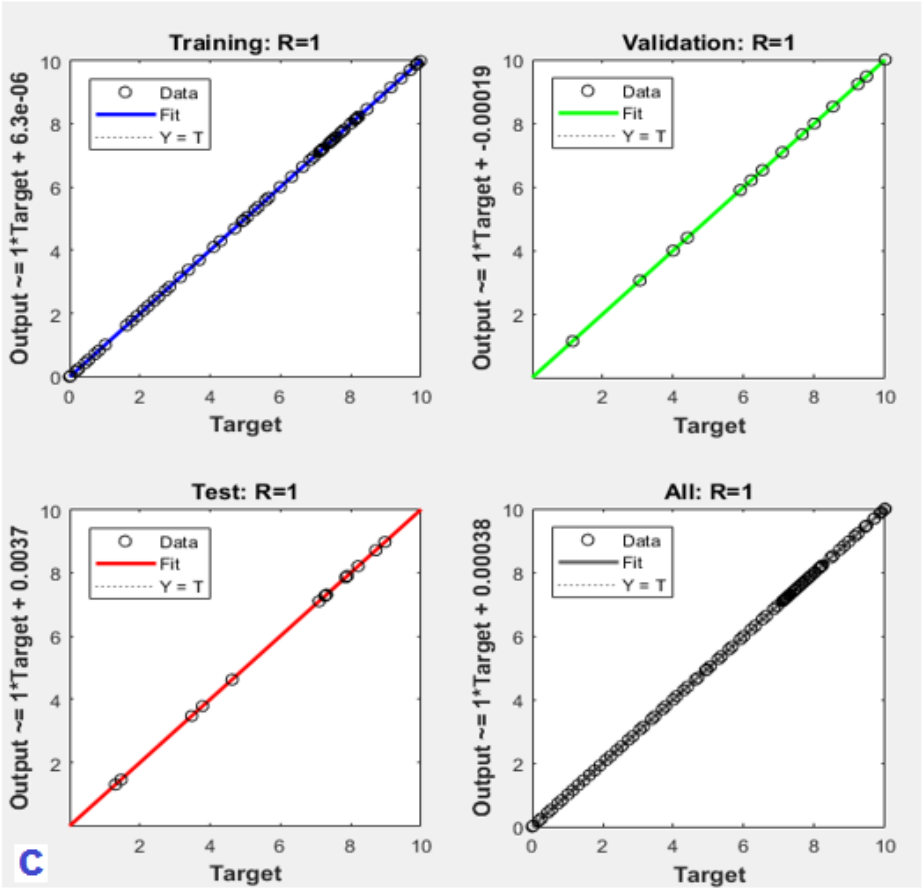

Figure 10. The network model with test training, validation, and the entire set with the prediction of a sample with an: (a) diameter of 1 mm lubricated sample, (b) diameter of 1 mm without lubrication, (c) diameter of 4 mm without lubrication

7. Conclusion

In this paper, the results of the effect of size and lubrication conditions on the copper microcylinder have been investigated. The results show that:

1) Flow stress size effect occurred in scaled-down cylinder compression whether using a lubricant or not. The yield strength decreased by about 30 MPa as the specimen size decreased from 8 mm to 1 mm. This can be explained by the dislocations in the specimens.

2) Tribology size effect occurred in scaled-down cylinder compression in the case of lubrication with oil. The friction factor increased by about 0.11 as the specimen size decreased from 8 mm to 1 mm. However, the tribology size effect is not found in the case without lubrication. This can be explained by the fraction of the real contact area under deformation.

8. References

[1] Geiger, M., Kleiner, M., Eckstein, R., Tiesler, N. and Engel, U. 2001. Microforming. CIRP Annals. 50: 445-462.

[2] Jiang, Z., Zhao, J., Lu, H., Wei, D., Manabe, K. I., Zhao, X. and Wu, D. 2017. Influences of temperature and grain size on the material deformability in microforming process. International Journal of Material Forming. 10: 753-764.

[3] Meng, B. and Chen, K. S. 2015. Ductile fracture and deformation behavior in progressive microforming. Materials and Design. 83: 14-25.

[4] Xu, Z., Qiu, D., Shahzamanian, M. M., Zhou, Z., Mei, D. and Peng, L. 2023. An improved springback model considering the transverse stress in microforming. International Journal of Mechanical Sciences. 241: 907-947.

[5] Gau, J. T., Principe, C. and Wang, J. 2007. An experimental study on size effects on flow stress and formability of aluminm and brass for microforming. Journal of Materials Processing Technology. 1843: 42-46.

[6] Meng, B., Cao, B. N., Wan, M., Xu, J. and Shan, D. B. 2020. Ultrasonic-assisted microforming of superalloy capillary: Modeling and experimental investigation. Journal of Manufacturing Processes. 57: 589-599.

[7] Wang, C., Wang, H., Chen, G., Zhu, Q., Zhang, G., Cui, L. and Zhang, P. 2020. Size effects affected uniaxial tensile properties and formability in rubber pad microforming process of pure nickel thin sheets. International Journal of Mechanical Sciences. 182: 105-157.

[8] Messner, A., Engel, U., Kals, R. and Vollertsen, F. 1994. Size effect in the FE-simulation of micro-forming processes. Journal of Materials Processing Technology. 45: 371-376.

[9] Chen, F. K., and Tsai, J. W. 2006. A study of size effect in micro-forming with micro-hardness tests. Journal of Materials Processing Technology.177: 146-149.

[10] Nanthakumar, S., Rajenthirakumar, D. and Avinashkumar, S. 2020. Influence of temperature on deformation behavior of copper during microextrusion process. Proceedings of the Institution of Mechanical Engineers, Part C. Journal of Mechanical Engineering Science. 234: 1797-1808.

[11] Ghassemali, E., Jarfors, A. E. W., Tan, M. J. and Lim, S. C. V. 2013. On the microstructure of micro-pins manufactured by a novel progressive microforming process. International journal of material forming. 6: 65-74.

[12] Krishnan, N., Cao, J. and Dohda, K. 2007. Study of the size effect on friction conditions in microextrusion experiments and analysis. Journal of Materials Processing Technology. 1:669-676.

[13] Vollertsen, F., Hu, Z., Niehoff, H. S. and Theiler, C. 2004. State of the art in micro forming and investigations into micro deep drawing. Journal of Materials Processing Technology. 151: 70-79.

[14] Vollertsen, F. and Hu, Z. 2006. Tribological size effects in sheet metal forming measured by a strip drawing test. CIRP Annals. 1: 291-294.

[15] Movahedian, S., Khamedi, R., Moradi, R. and Niknafs, H. 2021. Experimental and numerical analyses of carbon steel sheet metal forming process using strain rate dependent friction model. Materials Today: Proceedings. 42:1599-1607.

[16] Ebrahimi, R. and Najafizadeh, A. 2004. A new method for evaluation of friction in bulk metal forming. Journal of Materials Processing Technology. 2: 136-143.

[17] Wang, Z., Li, S., Wang, X., Cui, R. and Zhang, W. 2018. Modeling of surface layer and strain gradient hardening effects on micro-bending of non-oriented silicon steel sheet. Materials Science and Engineering. 711: 498-507.

[18] Aal, M.I.A.E., Mahallawy, N.E., Shehata, Hameed, F.A. Yoon, M., Lee, J.H. and Kim, H.S. 2010. Tensile properties and fracture characteristics of ECAP-processed Al and Al-Cu alloys. Metals and Materials International. 5: 709-716.

[19] Honarpisheh, M., Dehghani, M. and Haghighat, E. 2015. Investigation of Mechanical Properties of Al/Cu striped by equal channel angular rolling. Procedia Materials Science. 11: 1-5.

[20] Honarpisheh, M., Haghighat, E. and Kotobi, M. 2018. Investigation of residual stress and mechanical properties of equal channel angular rolled St12 strips. Procedia Materials Science. 10: 20-25.

[21] Toth, L., Arzaghi, Fundenberger, M., Beausir, J.J., B., Bouaziz, O. and Arruffat-Massion, R. 2009. Severe plastic deformation of metals by high-pressure tube twisting. Scripta Materialia. 3: 175-177.

[22] Nazari, F. and Honarpisheh, M. 2018. Analytical model to estimate force of constrained groove pressing process. Journal of Manufacturing Processes. 32: 11-19.

[23] Nazari, F., and Honarpisheh, M. 2019. Analytical and experimental investigation of deformation in constrained groove pressing process. Journal of Mechanical Engineering Science. 11: 3751-3759.

[24] Khanlari, H., and Honarpisheh, M. 2020. Investigation of microstructure, mechanical properties and residual stress in non-equal-channel angular pressing of 6061 aluminum alloy. Transactions of the Indian Institute of Metals. 5: 1109-1121.

[25] Khanlari, H., and Honarpisheh, M. 2023. An upper bound analysis of channel angular pressing process considering die geometric characteristics, friction, and material strain-hardening. CIRP Journal of Manufacturing Science and Technology. 41: 259-276.

[26] Moazam, M. A. and Honarpisheh, M. 2021. Improving the mechanical properties and reducing the residual stresses of AA7075 by combination of cyclic close die forging and precipitation hardening. Proceedings of the Institution of Mechanical Engineers, Part L: Journal of Materials: Design and Applications. 235: 542-549.

[27] Moazam, M. A., and Honarpisheh, M. 2020. The effects of combined cyclic close die forging and aging process on microstructure and mechanical properties of AA7075. Journal of Materials: Design and Applications. 234: 1242-1251.

[28] Moazam, M. A. and Honarpisheh, M. 2019. Ring-core integral method to measurement residual stress distribution of Al-7075 alloy processed by cyclic close die forging. Materials Research Express. 6: 86-93.

[29] Supriadi, S., Kristianto, H., Whulanza, Y., Saragih, A. S., Dhelika, R. and Latief, B. S. 2018. Fabrication of magnesium ecap based maxillary miniplate-typed implant through the method of micro forming .In IOP Conference Series: Materials Science and Engineering. 1: 12-37.

[30] Poggio, T., and Girosi, F. 1990. Networks for approximation and learning. Proceedings of the IEEE. 9: 1481-1497.

[31] Jiang, Z., Zhao, J., Lu, H., Wei, D., Manabe, K. I., Zhao, X. and Wu, D. 2017. Influences of temperature and grain size on the material deformability in microforming process. International Journal of Material Forming. 10: 753-764.

[32] Sanger, T. D. 1989. Optimal unsupervised learning in a single-layer linear feedforward neural network. Neural networks. 6: 459-473.

[33] Bin, G. U. O., Feng, G. O. N. G., Wang, C. J., and Shan, D. B. 2009. Flow stress and tribology size effects in scaled down cylinder compression. Transactions of Nonferrous Metals Society of China. 19: 516-520.

[34] Parasiz, S. A., Kutucu, Y. K. and Karadag, O. 2021. On the utilization of Sachs model in modeling deformation of surface grains for micro/meso scale deformation processes. Journal of Manufacturing Processes. 68: 1086-1099.

[35] Wang, C., Wang, H., Chen, G., Zhu, Q., Zhang, G., Cui, L. and Zhang, P. 2020. Size effects affected uniaxial tensile properties and formability in rubber pad microforming process of pure nickel thin sheets. International Journal of Mechanical Sciences. 182: 705-757.